ACS APPLIED MATERIALS & INTERFACES
Research Article
www.acsami.org

Ultrafiltration Membranes with a Thin Poly(styrene)-*b*-poly(isoprene) Selective Layer

Sarah E. Querelle,[‡] Elizabeth A. Jackson,[†] Edward L. Cussler,*[,‡] and Marc A. Hillmyer*[,†]

[†]Department of Chemistry and [‡]Department of Chemical Engineering and Materials Science University of Minnesota, Minneapolis, Minnesota 55455, United States

Supporting Information

ABSTRACT: Ultrafiltration membranes with an 80 nm thick block polymer derived selective layer containing 20 nm cylindrical pores were prepared by removing poly(lactide) (PLA) from a poly(styrene)-*b*-poly(isoprene)-*b*-poly(lactide) (PS-PI-PLA) film onto a microporous polymer support. The block polymer film adopted a core(PLA)-shell(PI) cylindrical morphology in which vertically-oriented PLA cylinders were degraded to leave PI-lined channels in a PS matrix. Thanks to the combination of PS and PI in the nanoporous matrix, chemical cross-linking was not needed to provide mechanical stability in the thin film. The membranes showed a hydraulic flux of 165 L m^{-2} h^{-1} bar^{-1} and were able to size-discriminate poly(ethylene oxide) (PEO) solutes in agreement with theoretical predictions.

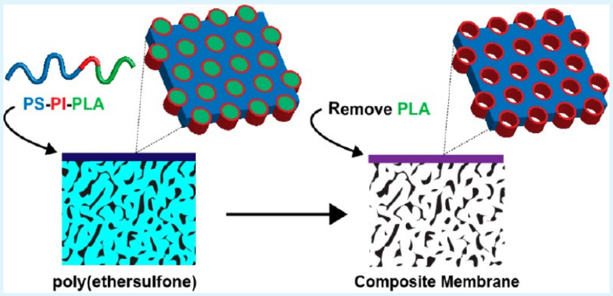

KEYWORDS: *triblock terpolymer, self-assembly, composite membrane, ultrafiltration, water treatment, size-selective rejection*

INTRODUCTION

Addressing the global water crisis requires new water purification processes that are more affordable and less energy intensive.[1−3] Nanoporous materials from block polymer precursors have received a tremendous amount of attention in the area of liquid separations[1,2,4−6] such as water filtration,[7,8] controlled drug delivery,[9,10] and virus filtration,[11,12] because of ideal attributes of controlled pore size, high porosity, tunable chemical, and mechanical properties.[13,14] Although polymer membranes have often been used for such applications, commercially available ultrafiltration membranes have suffered from a seemingly unbridgeable balance between high selectivity and high permeability.[15] Composite membranes containing thin nanoporous selective layers (< 100 nm thick) derived from block polymers have been predicted to surpass the current standard in ultrafiltration membranes in terms of both permeability and selectivity.[16]

Since the preparation of nanoporous materials from self-assembled block polymers reported by Lee et al.,[17,18] many groups have attempted to make selective nanoporous membranes.[19−30] Nanoporous materials made from traditional bulk block polymers have been too thick to provide useful permeabilities. Because of this, several strategies have been taken to create thinner block polymer membranes. "Composite" membrane ideas are attractive because they incorporate both a thin selective block polymer layer and a thicker, highly porous, mechanical support.[11−13,20−22] Composite membranes with thin selective layers have been prepared by spin-coating block polymer onto a sacrificial solid substrate; unfortunately, this technique requires the difficult transfer of the fragile thin film from the substrate to a porous support.[12,13] More recently, a phase inversion process has been used to create composite ultrafiltration membranes containing block polymer in both the thin self-assembled top layer and in the underlying non-solvent-induced microporous bottom layer.[21,22] However, the large amount of block polymer needed renders this strategy expensive. In summary, block polymer membranes have generally suffered from low permeabilities, difficult fabrication techniques, and high cost.

We present an alternative method to prepare ultrafiltration composite membranes with a self-assembled block polymer derived selective layer on top of a porous polymer support without tedious transfer steps. To obtain such a membrane, a thin film of poly(styrene)-*b*-poly(isoprene)-*b*-poly(lactide) (PS-PI-PLA) triblock terpolymer[31] solution was spin-coated directly onto a water-filled poly(ethersulfone) (PES) support membrane (Scheme 1). Previously, Phillip et al. demonstrated that PS-PLA copolymer films (4 μm) could be coated onto the surface of water filled supports from a water immiscible solution.[24] We have built on that strategy using spin coating to prepare thin (<100 nm) films of block polymer onto a water filled porous support. We posited that the joint presence of the rubbery poly(isoprene) (PI) and the glassy poly(styrene) (PS) within the ultimate nanoporous matrix would increase the robustness of the thin selective layer to avoid additional cross-linking steps. Previously, we demonstrated[32] that spin-coating a PS-PI-PLA from a chlorobenzene solution results in the spontaneous perpendicular orientation of core (PLA)−shell

Received: March 7, 2013
Accepted: May 3, 2013
Published: May 20, 2013

dx.doi.org/10.1021/am400847m | *ACS Appl. Mater. Interfaces* 2013, 5, 5044−5050

Scheme 1. Composite Membrane Fabrication

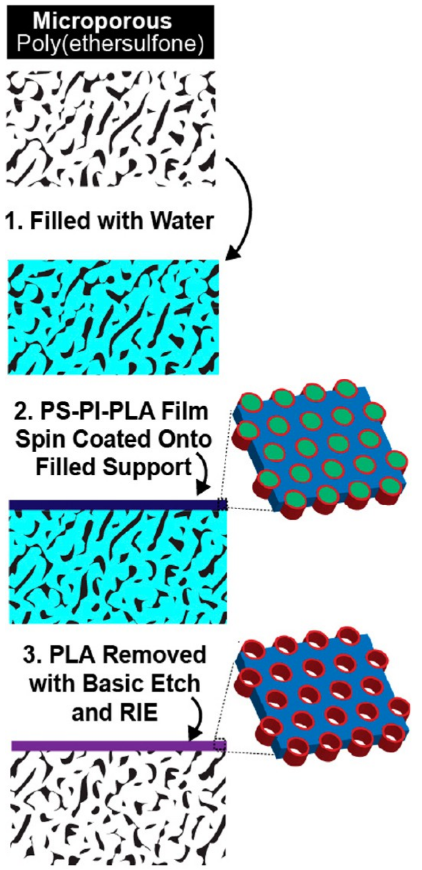

(PI) cylindrical domains without any additional annealing steps (Scheme 1, step 2). We found that nanopores could be created after basic hydrolysis of the PLA and a short oxygen (O_2) reactive ion etch (RIE), (Scheme 1, step 3). Here we show that by using the PS-PI-PLA block polymer we were able to create a thin nanoporous PS-PI selective layer that is mechanically robust enough to withstand both membrane fabrication and filtration. Furthermore, by decreasing the thickness of the selective layer to only 80 nm we have made a membrane with a competitive hydraulic permeability. As we demonstrate, this strategy represents a significant advance over our recently reported and related procedure based on the use of PS-PI-PS-PLA tetrablocks in terms of synthetic ease, molecular weight cutoff characteristics, and permeability.[33] In the following, we discuss composite membrane preparation, structure, and filtration performance of these new composite membranes.

PS-PI-PLA Morphology and Cylinder Orientation in Thin Films. The poly(styrene)-*b*-poly(isoprene)-*b*-poly(lactide) (PS-PI-PLA) block polymer used in this work was synthesized following a previously described procedure.[31] The PS-PI-PLA used has M_n values of 37, 7, and 21 kg mol^{-1} for the PS, PI, and PLA blocks, respectively, and a molar mass dispersity (Đ) of 1.13 (volume fractions are $f_{PS} = 0.62$, $f_{PLA} = 0.25$, and $f_{PI} = 0.13$). The bulk morphology of the triblock terpolymer was previously identified through a combination of SAXS and TEM experiments.[31] On the basis of our previous work,[31,32] we expect a hexagonally packed core−shell cylindrical morphology with PLA cylinders surrounded by a PI shell in a matrix of PS (Figure 1A). In this case, the SAXS data suggest a cylinder center-to-center distance of 68 nm, a PLA cylinder diameter of 34 nm, and a PI shell thickness of 3 nm.

TEM analysis of a drop-casted sample of PS-PI-PLA dried on a TEM grid confirmed the core−shell cylindrical morphology (Figure 1B, C). The PI domains, selectively stained with osmium tetraoxide (OsO_4), appear as dark shells separating the unstained PLA cylindrical cores from the unstained PS matrix. The cylinder center-to-center distance, the outer shell diameter, and the shell thickness are respectively 59 ± 5, 36 ± 1, and 9 ±

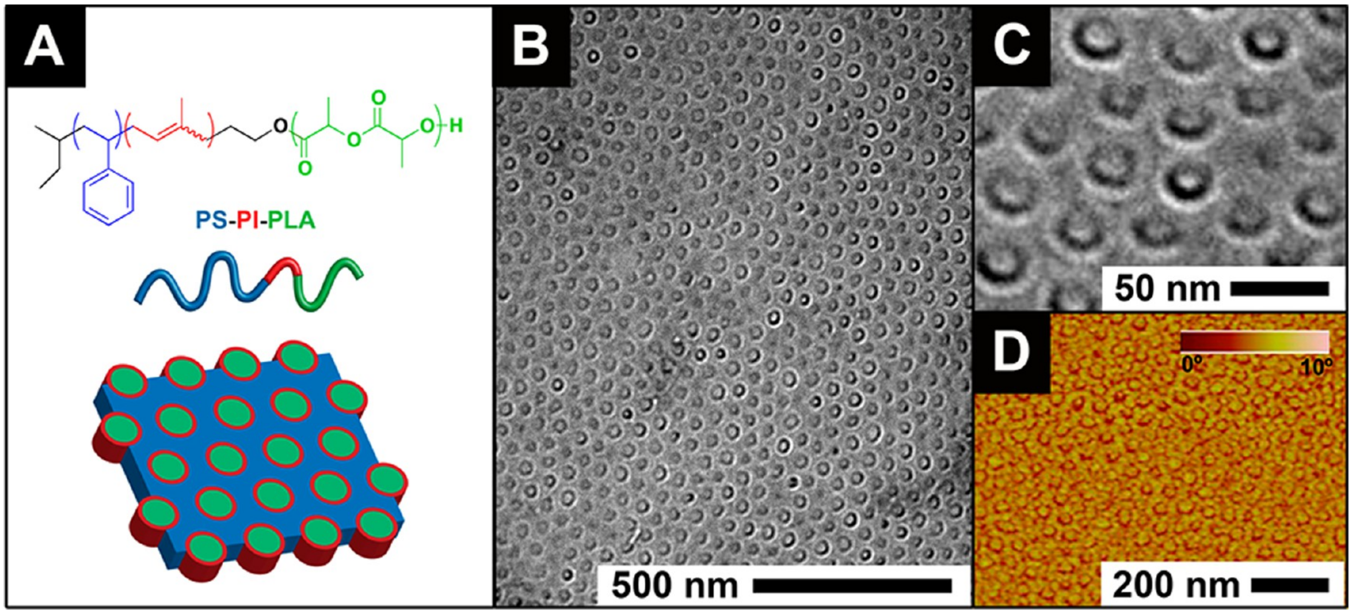

Figure 1. (A) Chemical structure and cartoon of PS-PI-PLA terpolymer (B) Representative TEM of the drop-cast PS-PI-PLA film showing a core (PLA)−shell (PI) cylindrical morphology. PI domains, selectively stained with OsO_4, form cylindrical shells surrounding PLA cores in a PS matrix. (C) Higher magnification of A. (D) Tapping-mode AFM phase image of a PS-PI-PLA thin film (thickness = 80 nm) on a hexamethyldisilazane (HMDS)-modified Si wafer. The PI rings are distinct from the PS and PLA domains because of mechanical and surface energy contrast.

1 nm. We believe that the apparent shell thickness determined from TEM (9 nm) is larger than that from SAXS (3.4 nm) because of OsO_4 infiltration into PLA or PS nanodomains.

We previously demonstrated that spin-coating a PS-PI-PLA thin film on a solid substrate results in a spontaneous perpendicular alignment of the PLA cylindrical domains without any additional thermal or solvent annealing.[32] In this work, we found that this is also true for 80 nm thin films of PS-PI-PLA cast onto hexamethyldisilazane (HMDS)-modified Si wafers (AFM in tapping mode, Figure 1D), onto NaCl single crystal disks (SEM after selectively degrading the PLA cylinders, Figure 2) and onto PES porous membranes imbibed with either water (SEM after PLA removal, Figure 4) or a dilute sodium hydroxide (NaOH) solution (AFM, see Figure S2 in the Supporting Information).

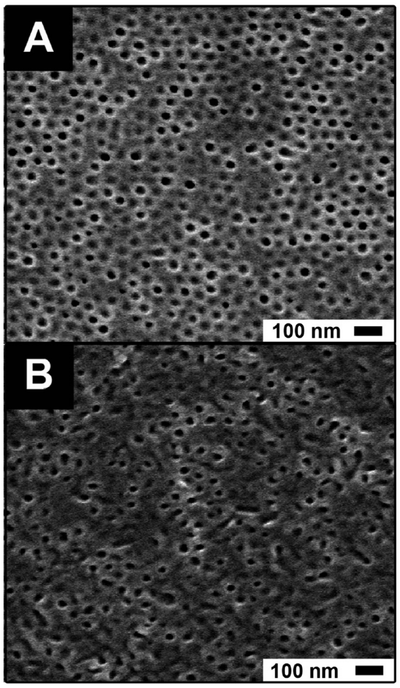

Figure 2. Representative SEM at the (A) top and (B) bottom of a PLA degraded PS-PI-PLA thin film prepared on a NaCl single crystal disk. Average pore diameter determined from SEM was 22 ± 3 nm; without RIE, the percentage of open pores was (A) 20% because of the polymer wetting (PS and/or PI) layer on the surface, and (B) 40% of open cylinders are compromised between top and bottom of film.

Composite Membrane Preparation and Structure. To directly prepare a PS-PI-PLA thin layer onto the PES porous membrane, we blocked the micropores in the PES support during the spin-coating by filling it with either pure water or a dilute NaOH solution. By spin-coating a solution of PS-PI-PLA in the water-immiscible solvent chlorobenzene, we limited mixing between the aqueous liquid filling the pores in the PES and the block polymer solution during the spin-coating process.

The SEM of the top surface of the PES support prior to PS-PI-PLA coating (Figure 3A) shows large micropores as expected. After coating the water-filled support with a thin PS-PI-PLA layer (Figure 3B), a film was successfully prepared over 11 cm^2 without any visible defects by SEM.

The cylindrical microdomains in the block polymer layer of the composite membrane were selectively etched using a 0.05 M NaOH solution. The selective layer of the composite membranes (Figure 4A) contains perpendicular cylindrical nanopores with diameters of 25 ± 3 nm. From the SEM image (Figure 4A), we estimated that 20% of the nanopores are fully "open" due to the presence of a polymer wetting layer at the surface, as was the case for PS-PI-PLA coated on the NaCl substrate.

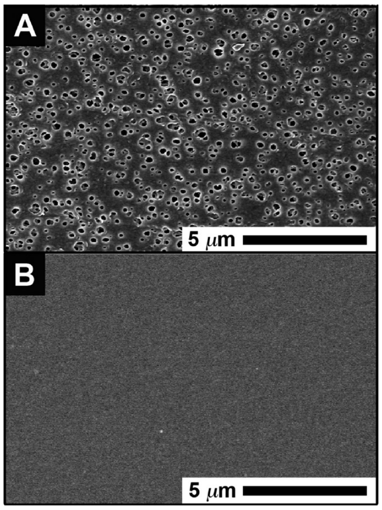

Figure 3. SEM of the top surface of the PES supporting membrane (A) before and (B) after spin coating the PS-PI-PLA solution onto a water-filled PES support.

To investigate the extent of vertical cylinder orientation through the film, we performed cross-sectional SEM analysis (Figures 4C, D). Uniform nanochannels perpendicular to the thin film surface can clearly be observed above the sharp boundary between the PES supporting membrane and the nanoporous layer. While the pores at the top of the selective layer are mostly perpendicular to the film surface, some appear to "tilt" within the film.

We turned to a two-step etching process to obtain more pores through the film. After basic etching to remove the PLA, the remaining polymer wetting-layer was removed by performing oxygen (O_2) reactive ion etching (RIE) for 10 s.[34] As shown in the Figure 4B, this additional etching increased the pore density and changed the average pore diameter to 20 ± 3 nm because of the creation of somewhat smaller pores during the RIE step. Consistent with the observed increase in flux observed after the RIE, we estimated that about 85% of the PLA cylindrical domains at the free surface are converted to pores using the two-step process.

Composite Membrane Performance. Unlike the PES porous support, the un-degraded composite membranes were impermeable to water at atmospheric pressure for 60 min and thus considered defect free. More than 10 mL of water passed through the bare PES support while no water passed through the un-etched block polymer-PES composite membrane.

The same membranes were then subjected to a mechanical stability test at a 0.1 bar pressure drop. Under these conditions, water began to emerge from the un-etched membrane after about 10 min (measured for membrane 2 in Table 1). After this 10 min lag, the average permeability of water across the membranes was about 26 L m^{-2} h^{-1} bar^{-1} (Table 1). Because industrial reverse osmosis and nanofiltration composite membranes[35] with a 200 nm selective layer present water permeabilities ranging from 1 to 14 L m^{-2} h^{-1} bar^{-1}, we conclude that the measured permeability is the result of water

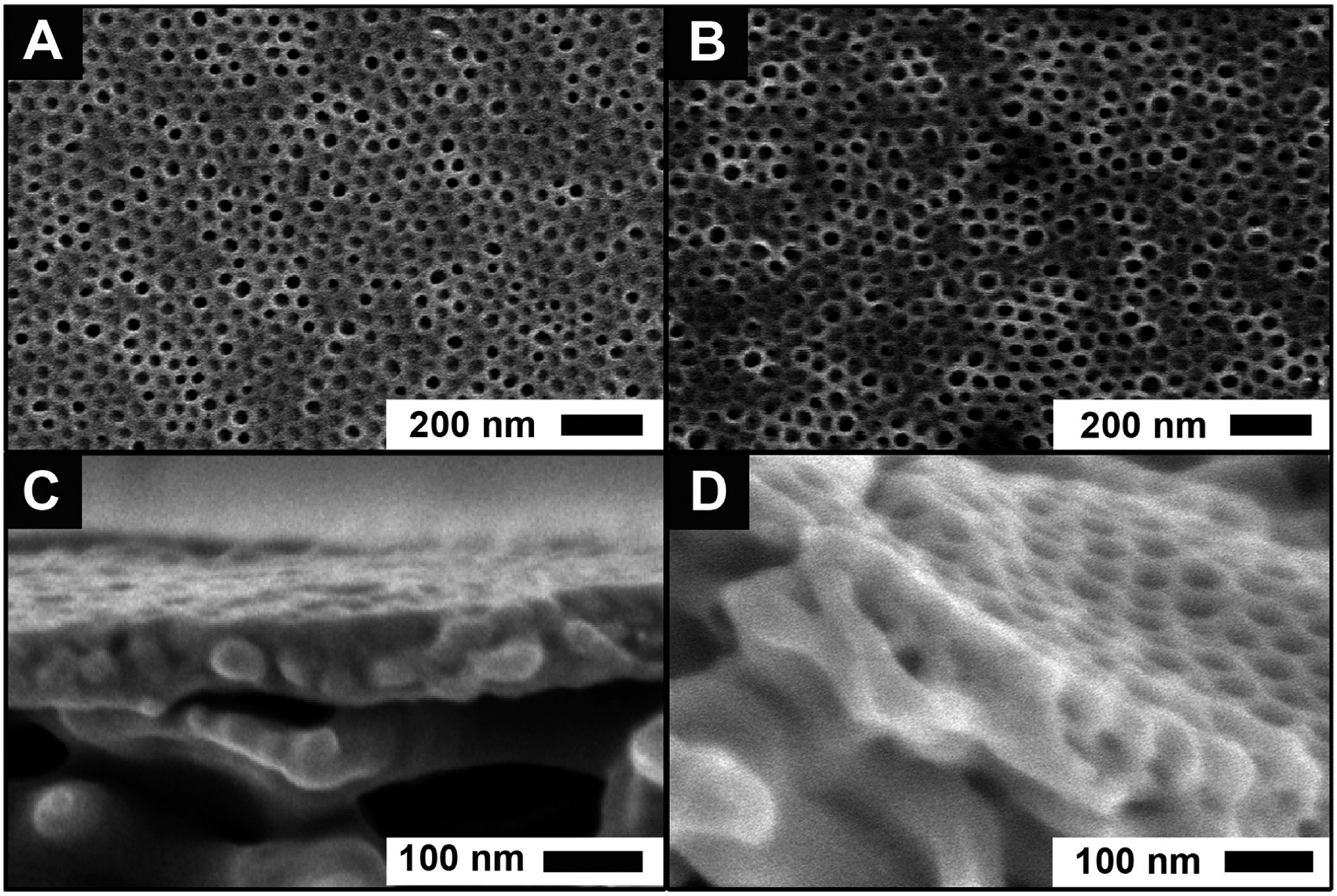

Figure 4. SEM of the nanoporous selective layer at the top surface of the composite membrane (A) after the PLA cylinder degradation using a 0.05 M NaOH solution in a 60/40 H_2O/MeOH (v/v) mixture and (B) after the same chemical etching followed by an O_2 RIE. (C, D) SEM cross-sectional micrographs of PLA-degraded PS-PI-PLA film on top of the PES supporting membrane.

Table 1. Hydraulic Permeability for Three Membranes Prepared Using the Same Procedure

	hydraulic permeability (L m^{-2} h^{-1} bar^{-1})[a]		
membrane	before PLA etching	after PLA etch	after O_2 RIE
1	29	30	202
2	21	47	158
3	28	44	133
average	26	40	165

[a] Measured at room temperature using a filtration cell at a stirring speed of 400 rpm. The permeating water was first collected to ensure a constant flow rate. The permeate mass was then recorded over time. The data in each column correspond to the membrane reference (1st column), the result before the PLA cylinders etching (2nd column), after the chemical degradation of the PLA domains (3rd column), and after the O_2 RIE (4th column).

diffusion through the more hydrophilic PLA domains of the unetched block polymer layer. The 10 min lag may be due to two factors; the diffusion in the ultrathin block polymer overlayer, and the convective flow in the underlying microporous support. Water diffusion in a polymer film is constant and associated with a time lag equal to $l^2/6D$, where l, the film the thickness, is 80 nm, and the diffusion coefficient, D, is approximated as 1×10^{-8} cm^2 s^{-1}. The estimated water diffusion lag is thus 0.001 s, much less than that observed. On the other hand, the time to push water through the support pores was estimated to be 7 minutes. Because this value was much closer to the experimental result of 10 min, we conclude that water filling the pores in the support pores causes most of the time lag (see the Supporting Information for more detail). The remaining time lag can be attributed to diffusion through the barrier layer.

After the defect and mechanical stability tests, the PLA cylinders in the composite membrane top layer were chemically etched with a dilute basic solution. Following water flushing of the membranes, the average water permeability was only 40 L m^{-2} h^{-1} bar^{-1}. However, after drying and subjecting these membranes to O_2 RIE, the same characterization gave an average of 165 L m^{-2} h^{-1} bar^{-1}. This two-step etching process significantly enhanced the pure water permeability.

The value of these membranes for ultrafiltration was further explored in rejection experiments using PEO standards (M_v ranging from 23.5 to 400 kDa) dissolved in HPLC grade water. Because the PES support has a molecular weight cut-off (MWCO) of 1000 kDa, these PEO samples are not retained by the support alone. PEO hydrodynamic radii (R_h) were calculated from the diffusion coefficient, D_{PEO} (R_{h_D}), and from the viscosity, η_o ($R_{h_{\eta_o}}$) (see the Supporting Information for calculations). In Figure 5, the percentages of rejected PEO by the composite membranes are plotted vs. λ (R_h/r_{pore}, where r_{pore} is the pore radius). From Figure 5, the PEO retention is nearly complete when the PEO hydrodynamic diameter ($2R_{h_D}$ = 21.2 nm; $2R_{h_{\eta_o}}$= 24.2 nm) is about the pore diameter (~20 nm). The theoretical rejection (dashed curve), based on a model

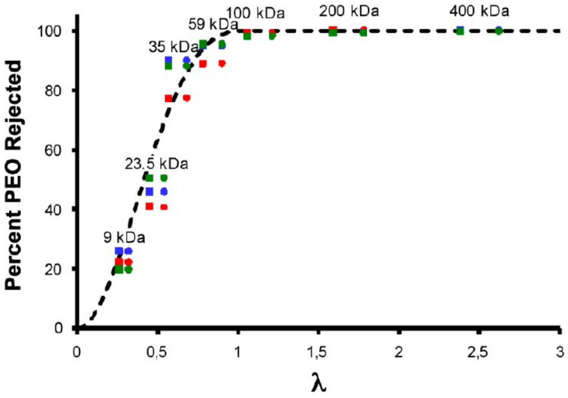

Figure 5. Percentages of rejected solute (for PEO samples with different molar masses) by the nanoporous composite membranes vs. λ; ratio between the PEO hydrodynamic radii and the nanopore radius (r_p= 10 nm). The filled squares and circles respectively correspond to the rejection data using λ calculated from R_{h_D} and $R_{h_{\eta o}}$. Different colors are attributed to different membranes, i.e., membrane 1 (red), membrane 2 (blue), and membrane 3 (green). The dashed curve corresponds to the predicted rejection curve (see the Supporting Information for calculations) based on the Bungay and Brenner model.[35,36].

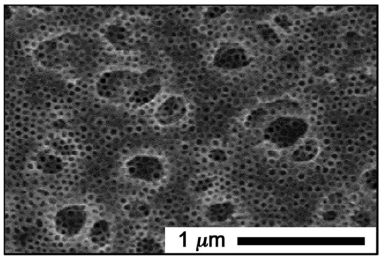

Figure 6. Overlay of the SEM surface micrographs of the nanoporous block polymer layer and the PES supporting material.

proposed by Bungay and Brenner[36,37] agrees with the experimental data and is sharper than for traditional phase inversion membranes (Figure 5).[38]

In comparison to previous work by Phillip et al.,[24] a thinner selective layer (80 nm vs. 4 μm) improves the hydraulic permeability by more than two orders of magnitude (165 L m^{-2} h^{-1} bar^{-1} vs. 1.15 L m^{-2} h^{-1} bar^{-1}). Because nanoporous films thinner than 500 nm should have little contribution to the fluid flow through the composite membrane,[39] we expect that the theoretical composite membrane permeability will depend only on the support membrane permeability and the fraction of the support pores that are covered by open nanopores. For the ideal case, where all PLA (f_{PLA}= 0.25) is removed, this would mean that only 25% of the support surface pores are accessed by the nanopores. In this case the permeability should be the support permeability, 3400 L m^{-2} h^{-1} bar^{-1}, multiplied by the volume fraction of open pore volume, 0.25, or 850 L m^{-2} h^{-1} bar^{-1} (= 0.25 × 3400 L m^{-2} h^{-1} bar^{-1}). From our SEM analysis, we estimate that only 34% of the pores are available due to some PLA domains being trapped between the film top and bottom. The trapped PLA domains further decrease the estimate to 289 L m^{-2} h^{-1} bar^{-1} (= 0.25 × 0.34 × 3400 L m^{-2} h^{-1} bar^{-1}). This estimate is relatively close to our measured permeability of 165 L m^{-2} h^{-1} bar^{-1}. Thus the membranes developed in this work sustain the very high selectivity possible with the block polymer based membrane developed earlier, and they also achieve a much higher permeability. The obvious question is how much more this permeability could be increased if we made further improvements to the selective membrane itself.

Outlook. There are three ways in which we can imagine improving these composite membranes. One is to use a supporting membrane with a more open surface structure. We suspect that this could lead to marginal improvements; however, the limiting resistance to mass transfer at the moment is almost exclusively in the thin block copolymer film and that changes in support are unlikely to produce major gains. Second, we could also imagine making the membrane thinner; however, thinner than perhaps 20 nm would be at about the practical limit. Thus, we could get only a four-fold improvement in flux in this way. Still, this idea has merit and is worth pursuing in future work. The third way is to increase the fraction of open pores. Previously we have found that spin coating block copolymers and evaporating the solvent rapidly results in spontaneous perpendicular orientation of the PLA cylinders independent of the substrate and thickness used.[24] By using thinner films and reactive ion etching we have been able to increase the number of cylinders that span the entire film. A more finely tuned solvent casting step that allows the block polymer cylindrical domains to align more vertically would also enhance the pore density. Although this may prove challenging, the maximum gain is probably on the order of a factor of 2 and certainly no more than a factor of 3.

■ CONCLUSIONS

In conclusion, nanoporous composite membranes with an 80 nm selective layer and 20 nm cylindrical pores were prepared using a self-assembled PS-PI-PLA block polymer. The thin film was directly deposited at the surface of a porous support and adopted a core(PLA)−shell(PI) cylindrical morphology. The added PI block increases the mechanical robustness of the mostly PS film. The PI pore "coatings" could potentially also permit a variety of chemical transformations, including hydrophilic modification to reduce fouling and increase flux.[32] After the etching of the PLA cylinders, highly size selective membranes with a high hydraulic permeability of 165 L m^{-2} h^{-1} bar^{-1}, comparable to current commercial membranes, were obtained. These membranes have a very sharp molecular weight cut-off because of the size-calibrated nanochannels spanning the thin selective layer.

■ EXPERIMENTAL DETAILS

Triblock Terpolymer. The PS-PI-PLA was synthesized using the combination of anionic polymerizations and a controlled ring-opening polymerization.[27] The block polymer chemical structure and bulk morphology were previously determined through a combination of ^{1}H NMR spectroscopy, SEC, SAXS, and TEM.[31,32] The TEM characterization was performed on a Jeol 1210 transmission electron microscope operating at 120 kV. To generate electron density contrast, the PI blocks were selectively stained with OsO_4 vapor.

Preparation of PS-PI-PLA Thin Films. In all cases, a 2 wt % solution of PS-PI-PLA in chlorobenzene was spin-coated at 2000 rpm. Films were coated onto either HMDS-modified Si wafers, NaCl crystals, or porous PES membranes. The PS-PI-PLA solution was always dispensed in the center of the sample after starting the spin coater. For the preparation of the HMDS modified Si substrate, the Si wafer was cleaned of any oxide layer by immersion in 50/50 v/v H_2SO_4/H_2O_2 for 30 min. After being rinsed with water and ethanol and dried with nitrogen, the wafers were stored overnight in a 0.5% HMDS solution in toluene. Finally, the substrate was rinsed with toluene, dried with nitrogen, and stored under reduced pressure. For the support membrane coating, the PES membrane attached to the Teflon sheet was immersed in deionized water or a 0.05 M aqueous NaOH solution for at least 30 s, and then shaken to remove excess liquid and taped onto the center shaft of the spin coater equipped with a metal disk (see Figure S1 in the Supporting Information). Finally, the spin coating was performed for 2 min using 0.5 mL of PS-PI-PLA solution. Film thicknesses of PS-PI-PLA films spin coated on Si wafers were measured by spectroscopic ellipsometry using a J. A. Woolam, EC-2000 ellipsometer, with incident angles of 75 and 90°, and laser wavelengths between 400 and 1100 nm. Other PS-PI-PLA film thicknesses were estimated by cross-sectional SEM analysis. AFM surface morphological analyses were performed using a Digital Instruments Nanoscope III multimode system with Olympus tapping-mode etched silicon probes (Veeco Instruments) (force constant ~42 N/m, resonance frequency 200−400 kHz).

PLA Degradation. Samples were first exposed to a 0.05M NaOH solution in a water/methanol mixture (60/40 : v/v) for 45 min, and then rinsed in a base-free H_2O/MeOH solution (60/40 : v/v) for 15 min. When the sample was a composite membrane, the membrane was in the filtration module during the chemical etching and H_2O/MeOH rinsing. The etching solution was fully purged from the composite membranes by driving water through at a gauge pressure of 0.4 bar. The O_2 RIE was performed on a Surface Technology Systems Model 320 batch plasma etcher. A process pressure of 70 mTorr and a chamber power of 60W were used for 10s. SEM analyses were performed on a Hitachi S-900 FE-SEM instrument using a 2 or 3 kV accelerating voltage. Prior to SEM characterization, samples were coated with a 30 Å thick platinum layer via direct sputtering using a VCR ion beam sputter coater. Cross-sections for SEM analysis were prepared by breaking the samples under liquid nitrogen.

Composite Membrane Characterization. Unetched membranes were placed in an Amicon 8010 stirred cell filled with water to check if the PS-PI-PLA film coating on PES support was defect-free. More than 10 mL of water permeated through the uncoated PES porous support in 30 min at atmospheric pressure. The unetched composite membranes were considered defect-free if no water permeated in an hour at atmospheric pressure.

For the mechanical stability test, 0.1 bar nitrogen pressure drop was applied to the unetched membranes, the time needed for water to emerge from the membrane was measured, and the average flux of water across the membranes was then recorded.

Water flow experiments were performed in the Amicon 8010 filtration cell at room temperature and a stirring speed of 400 rpm.

The membranes were challenged in rejection experiments with 1.5 g L^{-1} PEO solutions in HPLC grade water. Solutions of individual PEO samples with different molar masses (M_v = 9.0, 23.5, 35.0, 59.0, 100.0, 200.0, and 400.0 kg mol^{-1}) were passed through the membrane at a constant pressure drop (~0.15 bar) and stirring speed (400 rpm). Between each measurement with a PEO solution, the membrane was flushed with HPLC water. Concentrations of the collected solutions were determined from data obtained using a differential refractometer (Optilab rEX, Wyatt Technology Corporation). For every analysis, 1 mL of collected solution was diluted with 2 mL of HPLC water, passed through a syringe filter (Acrodisc, PTFE, 0.2 μm, 25 mm, Pall Corporation), and injected into the refractometer using a 1 mL loop and a 1 mL min^{-1} flow (426 HPLC pump, Alltech).

■ ASSOCIATED CONTENT

Ⓢ Supporting Information

Further details concerning the experimental section and calculations. This material is available free of charge via the Internet at http://pubs.acs.org.

■ AUTHOR INFORMATION

Corresponding Author

*E-mail: cussler@umn.edu (E.L.C.); hillmyer@umn.edu (M.A.H.).

Author Contributions

All authors had significant scientific contributions to this work. The experimental work was completed by S.E.Q. with the exception of TEM characterization in the Supporting Information, which was acquired by E.A.J. An initial draft of the manuscript was prepared by S.E.Q. E.A.J. made significant contributions to the organization, writing, and figures.

Notes

The authors declare no competing financial interest.

■ ACKNOWLEDGMENTS

This work was supported primarily by the National Science Foundation through the University of Minnesota MRSEC under Award DMR-0819885. Support for this work was also provided by the National Science Foundation under Award DMR-1006370. The authors thank Marc Rodwogin for the synthesis and characterization of the triblock terpolymer used in this work. The authors also thank Andrew Baruth for the O_2 RIE experiments. S.E.Q. thanks the late Gary M. Hendel for his contributions to the writing of this manuscript.

■ REFERENCES

(1) *Water for People, Water for Life—The United Nations World Water Development Report*; World Water Assesment Program of the United Nations Educational Scientific and Cultural Organization (UNESCO) and Berghahn Books: Colombella, Italy, 2003.

(2) Lenton, R.; Wright, A. M.; Lewis, K. *UN Millenium Project 2005: Health Dignity and Development: What Will It Take? Task Force on Water and Sanitation*; Earthscan: London, 2005.

(3) Singh, R. *Hybrid Membrane Systems for Water Purification: Technology, Systems Design and Operation*; Elsevier:Amsterdam, The Netherlands, 2006.

(4) Hoek, E. M. V.; Jawor, A. Nanofiltration Separations. In *Encyclopedia of Nanoscience and Nanotechnology*; Schwarz, J., Contescu, C., Putyera, K., Eds.; Marcel Dekker: New York, 2004; Vol. *1*, p 2399.

(5) Ulbricht, M. *Polymer* **2006**, *47*, 217−2262.

(6) Olson, D. A.; Chen, L.; Hillmyer, M. A. *Chem. Mater.* **2008**, *20*, 869−890.

(7) Shannon, M. A.; Semiat, R. *MRS Bull.* **2008**, *33*, 9−15.

(8) Shannon, M. A.; Bohn, P. W.; Elimelech, M.; Georgiadis, J. G.; Mariñas, B. J.; Mayes, A. M. *Nature* **2008**, *452*, 301−310.

(9) Nuxoll, E. E.; Hillmyer, M. A.; Wang, R.; Leighton, C.; Siegel, R. A. *ACS Appl. Mater. Interfaces* **2009**, *1*, 888−893.

(10) Yang, S. Y.; Yang, J.; Kim, E. -S.; Jeon, G.; Oh, E. J.; Choi, K. Y.; Hahn, S. K.; Kim, J. K. *ACS Nano* **2010**, *4*, 3817−3822.

(11) Yang, S. Y.; Ryu, I.; Kim, H. Y.; Kim, J. K.; Jang, S. K.; Russell, T. P. *Adv. Mater.* **2006**, *18*, 709−712.

(12) Yang, S. Y.; Park, J.; Yoon, J.; Ree, M.; Jang, S. K.; Kim, J. K. *Adv. Funct. Mater.* **2008**, *18*, 1371−1377.

(13) Hillmyer, M. A. *Adv. Polym. Sci.* **2005**, *190*, 137−181.

(14) Jackson, E. A.; Hillmyer, M. A. *ACS Nano* **2010**, *4*, 3548−3553.

(15) Mehta, A.; Zydney, A. L. *J. Membrane Sci.* **2005**, *249*, 245−249.

(16) Pendergast, MT. M.; Hoek, E. M. V. *Energy Environ. Sci.* **2011**, *4*, 1946−1971.

(17) Lee, J. S.; Hirao, A.; Nakahama, S. *Macromolecules* **1988**, *21*, 274−276.

(18) Lee, J. S.; Hiro, A.; Nakahama, S. *Macromolecules* **1989**, *22*, 2602−2605.

(19) Thurn-Albrecht, T.; Steiner, R.; DeRouchey, J.; Stafford, C. M.; Huang, E.; Bal, M.; Tuominen, M.; Hawker, C. J.; Russell, T. P. *Adv. Mater.* **2000**, *12*, 787−791.

(20) Zalusky, A. S.; Olayo−Valles, R.; Wolf, J. H.; Hillmyer, M. A. *J. Am. Chem. Soc.* **2002**, *124*, 12761−12773.

(21) Hedrick, J.; Labadie, J.; Russell, T.; Hofer, D.; Wakharker, V. *Polymer* **1993**, *34*, 4717−4726.

(22) Olayo−Valles, R.; Lund, M. S.; Leighton, C.; Hillmyer, M. A. *J. Mater. Chem.* **2004**, *14*, 2729−2731.
(23) Zhang, M.; Yang, L.; Russell, T. P. *Adv. Mater.* **2007**, *19*, 1571−1576.
(24) Phillip, W. A.; O'Neill, B.; Rodwogin, M.; Hillmyer, M. A.; Cussler, E. L. *ACS Appl. Mater. Interfaces* **2010**, *2*, 847−853.
(25) Peinemann, K.; Abetz, V.; Simon, P. F. W. *Nat. Mater.* **2007**, *6*, 992.
(26) Phillip, W.A.; Dorin, R.M.; Werner, J.G.; Hoek, E.M.V.; Wiesner, U.; Elimelech, M. *Nano Lett.* **2011**, *11*, 2892−2900.
(27) Phillip, W. A.; Amendt, M.; O,Neill, B.; Chen, L.; Hillmyer, M. A.; Cussler, E.L. *ACS Appl. Mater. Interfaces* **2009**, *1*, 472−480.
(28) Uehara, H.; Kakiage, M.; Sekiya, M.; Sakuma, D.; Yamonobe, T.; Takano, N.; Barraud, A.; Meurville, E.; Ryser, P. *ACS Nano* **2009**, *3*, 924−932.
(29) Liu, G.; Ding, J.; Stewart, S. *Angew. Chem., Int. Ed.* **1999**, *38*, 835−838.
(30) Li, X.; Fustin, C.-A.; Lefevre, N.; Gohy, J.-F.; De Feyter, S.; De Baerdemaeker, J.; Egger, W.; Vankelecom, I. F. J. *J. Mater. Chem.* **2010**, *20*, 4333−4339.
(31) Bailey, T. S.; Rzayev, J.; Hillmyer, M. A *Macromolecules* **2006**, *39*, 8772−8781.
(32) Kubo, T.; Wang, R. F.; Olson, D. A.; Rodwogin, M. A.; Hillmyer, M. A. *Appl. Phys. Lett.* **2009**, *93*, 133112(1−3).
(33) Jackson, E. A.; Lee, Y.; Hillmyer, M. A. *Macromolecules* **2013**, *46*, 1484−1491.
(34) Kubo, T.; Parker, J. S.; Hillmyer, M. A.; Leighton, C. *Appl. Phys. Lett.* **2007**, *90*, 233113.
(35) *Dow Water and Process Solutions Home page, Support and Training, Product Manuals, Dow Filmtec Reverse Osmosis Technical Manual*; http://www.dowwaterandprocess.com/ (accessed Jun 27, 2011).
(36) Bungay, P. M.; Brenner, H. *Int. J. Multiphase Flow* **1973**, *1*, 25−56.
(37) Silva, V.; Prádanos, P.; Palacio, L A.; Hernández, A. *Desalination* **2009**, *246*, 233−240.
(38) Phillip, W. A.; Amendt, M.; O,Neill, B.; Chen, L.; Hillmyer, M. A.; Cussler, E.L. *ACS Appl. Mater. Interfaces* **2009**, *1*, 472−480.
(39) Phillip, W. A. Block Polymer Membranes for Selective Separations. *Ph.D. Dissertation*, University of Minnesota, Twin Cities, MN, 2009.